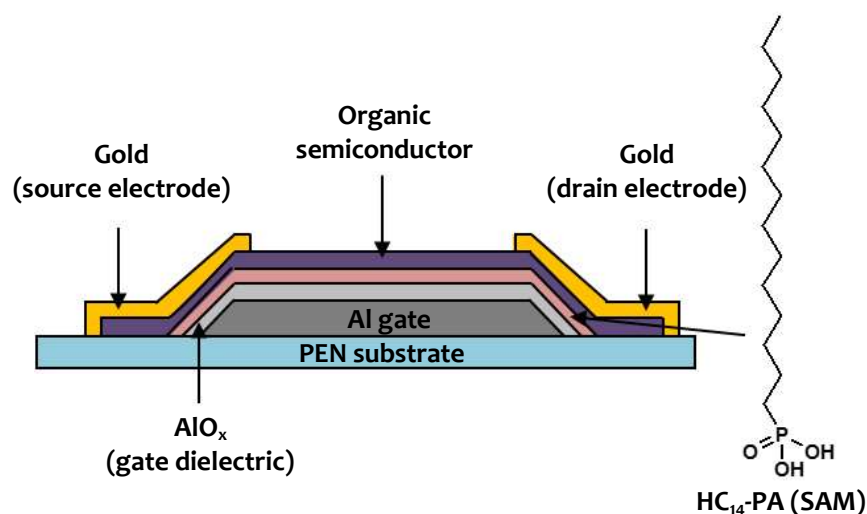


## Flexible Low Voltage Organic TFTs

Organic TFTs are getting a lot of attention for use in future flexible and large-area electronics due to its benefits such as easy processing, low-temperature processing capabilities, and compatibility with flexible plastic substrates. The low-voltage organic TFTs are essential to minimize the power consumption. The architecture and operation of organic TFTs are already discussed in Section 2.4 followed by a discussion of the fabrication and electrical characterization of p-channel organic TFT on rigid Si substrates. In this Chapter, high-performing organic TFTs fabricated on flexible plastic substrates are demonstrated and discussed.

### 3.1 FLEXIBLE ORGANIC TFTs

The bottom-gate-top-contact (inverted staggered) structure is used for the fabrication of organic TFTs in this study. The advantages of using this structure are to have a smooth dielectric/semiconductor interface, and smaller contact resistance than that of coplanar structure. The schematic diagram of fabricated organic TFTs is shown in Figure 3.1.



**Figure 3.1** :Schematic diagram of Organic TFTs Fabricated during this Study with the Chemical structure of the SAM i.e. Tetradecylphosphonic Acid

All organic TFTs were fabricated on flexible PEN plastic substrates. The photograph of PEN substrate before processing is shown in Figure 3.2. The polyethylene naphthalate film (Teonex® Q65 PEN) was 125- $\mu\text{m}$ -thick, transparent, resistant to organic solvents and chemicals, durable, electrically insulated, resistant and stable to heat up to 200°C [Teijin DuPont, 2014]. This PEN substrate was provided by William A. MacDonald, DuPont Teijin Films, Wilton, United

Kingdom. The fabricated organic TFT consists of aluminium as the gate electrode, combination of  $\text{AlO}_x$  and a SAM as the dielectric layer, organic semiconductor as the active material, and gold as source and drain contacts (see Figure 3.1).

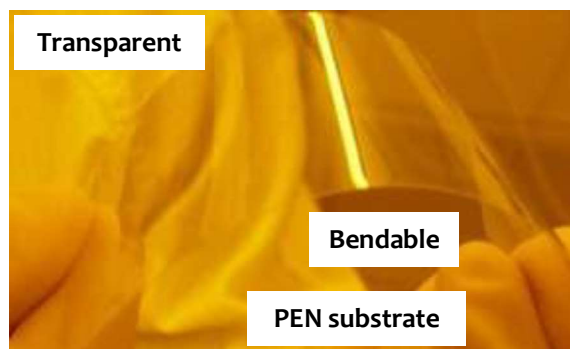


**Figure 3.2 :**Photograph of a Fresh Polyethylene Naphthalate Substrate

## 3.2 ORGANIC SEMICONDUCTORS INVESTIGATED

The six promising hole and electron transport organic semiconductors used for the fabrication of p-channel and n-channel devices respectively are introduced here.

### 3.2.1 Hole-transport Semiconductors

The four hole-transport organic semiconductors used for the studies conducted for this thesis work are pentacene [Yen-Yi *et al*, 1997], dinaphtho[2,3-b:2',3'-f]thieno[3,2-b]thiophene abbreviated as DNNT [Yamamoto and Takimiya, 2007], 2,9-didecyl-DNNT ( $\text{C}_{10}$ -DNNT) [Kang *et al*, 2011] and 2,9-diphenyl-DNNT (DPh-DNNT) [Niimi *et al*, 2011].  $\text{C}_{10}$ -DNNT and DPh-DNNT are derivatives of DNNT, showing better performance in TFT devices. All of these organic semiconductors have HOMO level in the range of 5 eV to 5.44 eV near to the Fermi level of gold (5.1 eV), which is used as a source/drain electrodes in TFT devices, making them suitable for hole injection.

Pentacene is an extensively studied organic semiconductor for p-channel organic TFTs [Yen-Yi *et al*, 1997; Kalb *et al*, 2007; Wang *et al*, 2008; Zhang *et al*, 2009; Häusermann and Batlogg, 2011; Lu *et al*, 2011; Yan *et al*, 2011]. The chemical structure of this semiconductor is given in Figure 3.3(a). It has a HOMO-LUMO energy gap of  $\sim 2.0$  eV and HOMO energy level of  $\sim 5.0$  eV. It has consistently shown the field-effect mobility values in the range of  $\sim 0.002$   $\text{cm}^2/\text{Vs}$  to  $\sim 10$   $\text{cm}^2/\text{Vs}$  in the last three decades [Horowitz *et al*, 1992; Wei *et al*, 2011]. The field-effect mobility value of  $\sim 1.0$   $\text{cm}^2/\text{Vs}$  was reported for the TFTs on Si/SiO<sub>2</sub> substrates as early as in year 1997 for devices operating at 80 V [Lin *et al*, 1997]. The techniques such as annealing before semiconductor deposition and treatment of the interface of dielectric with SAM has been used to improve the device properties and to reduce the hysteresis in the devices due to any -OH dangling bonds or moisture [Gundlach *et al*, 1997; Guo *et al*, 2006; Zschieschang *et al*, 2010; Colleaux *et al*, 2011]. The effect of annealing the pentacene based TFTs after its fabrication is reported to improve the performance of devices, when temperature of annealing is below the critical temperature (45°C) due to improvement in the grain-size of pentacene [Guo *et al*, 2006]. The substrate temperature (while depositing the semiconductor) and thickness of semiconductor film also play a crucial role in demonstrating better performance in devices and it has been optimized to 60°C and 30 nm respectively [Gundlach *et al*, 1997]. The substrate temperature and deposition rate both play an important role in deciding the grain size of multicrystalline pentacene films [Gundlach *et al*, 1997; Knipp *et al*, 2003]. Higher grain size results in less number of boundaries eventually

leading to high field-effect mobility in devices. High field-effect mobility values more than 2  $\text{cm}^2/\text{Vs}$  are reported for pentacene TFTs, however, most of these studies are done either on rigid substrates or for devices operating at high voltages mostly between 20 V to 100 V. To reduce the operating voltage in the devices, high-k gate dielectric materials such as hafniumdioxide ( $\text{HfO}_2$ ), silicon nitride ( $\text{Si}_3\text{N}_4$ ), and aluminiumdioxide ( $\text{Al}_2\text{O}_3$ ), deposited by techniques such as sputtering and chemical vapor deposition (CVD) and ALD are used in the gate dielectric as pristine or in combination with polymer or SAM layers [Knipp *et al*, 2003; Zhang *et al*, 2007; Tiwari *et al*, 2009]. A very thin buffer layer of  $\sim 20$  to 30 nm of polymer on the top of these inorganic dielectrics is used to fabricate rigid devices with low operating voltage of about 3.0 V with field-effect mobility of 2  $\text{cm}^2/\text{Vs}$  [Hwang *et al*, 2006; Tiwari *et al*, 2009]. The thickness of these buffer layers are limited by processability issues. Hence, the overall thickness of the dielectric cannot be reduced to less than few tens of nanometers, limiting the further increase in the capacitance density. These techniques used for depositing high-k dielectrics are primarily used in microelectronics industry and require high capital investments. To reduce the cost of processing and also to introduce the flexibility in devices, solution processable polymer gate dielectrics are used. Using the polymer gate dielectric layers (PVP and a PVP-based copolymer), which are also known to provide smooth surface with less charge trapping, field-effect mobility as high as 3  $\text{cm}^2/\text{Vs}$  was achieved from TFTs on rigid Si substrate operating at 30 V [Klauk *et al*, 2002]. A very high field-effect mobility of 8.85  $\text{cm}^2/\text{Vs}$  for operating voltage of 6.0 V was reported for pentacene TFTs fabricated on glass substrate with a solution-processed barium titanate (250 nm thick) as gate dielectric [Wei *et al*, 2011]. Though polymer gate dielectrics are favorable to achieve flexibility, thick layers of these materials are often required to keep the leakage currents low. High thickness of these polymers is a hindrance in obtaining high capacitance density because most of these polymers offer low dielectric constants. To overcome these issues, a combination of a very thin high-k and ultrathin SAM proved to be excellent way to produce a gate dielectric thickness of a few nanometers. One such demonstrated technique to fabricate pentacene TFTs on flexible substrates operating at low voltages (3.0 V) and exhibiting field-effect mobility value ( $\sim 1$   $\text{cm}^2/\text{Vs}$ ), has been reported by using a thin dielectric consisting of combination of oxygen plasma grown  $\text{AlO}_x$  and a phosphonic acid SAM [Zschieschang *et al*, 2010].

The chemical structure of DNNT is given in Figure 3.3(b). DNNT is a thienoacene originated organic semiconductor, which shows remarkably high field-effect mobility in p-channel organic TFTs. This semiconductor has an energy gap of  $\sim 3\text{eV}$  and a HOMO energy level of  $\sim 5.44$  eV and it shows quite impressive air and thermal stability [Yamamoto and Takimiya, 2007; Kang *et al*, 2011; Niimi *et al*, 2011]. DNNT was synthesized and reported to have effective field-effect mobility in range of 0.73  $\text{cm}^2/\text{Vs}$  to 2.9  $\text{cm}^2/\text{Vs}$  (depending on different surface treatments and substrate temperature) for TFTs fabricated on Si/SiO<sub>2</sub> substrates [Yamamoto and Takimiya, 2007]. TFTs with DNNT on flexible plastic substrates have shown a field-effect mobility of 2  $\text{cm}^2/\text{Vs}$ , and very high current on/off ratios of  $10^8$  [Zschieschang *et al*, 2011].

The chemical structure of C<sub>10</sub>-DNNT is given in Figure 3.3(c). This semiconductor has an energy gap of  $\sim 3$  eV and a HOMO energy level  $\sim 5.38$  eV [Hofmockel *et al*, 2013]. The synthesis of C<sub>10</sub>-DNNT and the field-effect mobility of 8  $\text{cm}^2/\text{Vs}$  for the TFTs with this semiconductor on octadecyltrichlorosilane (ODTS) treated Si/SiO<sub>2</sub> substrates were reported by Niimi [Niimi *et al*, 2011]. C<sub>10</sub>-DNNT can be deposited either by vacuum evaporation or by solution processing. Field-effect mobility as high as 10.7  $\text{cm}^2/\text{Vs}$  was reported for TFTs on rigid glass substrates with C<sub>10</sub>-DNNT deposited by edge-cast solution crystallization process on high-k Al<sub>2</sub>O<sub>3</sub> gate dielectric deposited by ALD ( $\sim 100$  nm thick) and treated with silane SAM [Ou-Yang *et al*, 2012]. The field-effect mobility achieved by C<sub>10</sub>-DNNT TFTs depends on the substrate temperature during deposition of active layer by vacuum evaporation, and it is in a range of 6  $\text{cm}^2/\text{Vs}$  to 8.5  $\text{cm}^2/\text{Vs}$  when substrate temperature is in the range of 40°C to 80°C, respectively [Hofmockel *et al*, 2013]. This semiconductor also exhibits high field-effect mobility up to 4.3  $\text{cm}^2/\text{Vs}$  on flexible plastic

substrates [Doi *et al*, 2012; Zschieschang *et al*, 2012]. It can be seen that C<sub>10</sub>-DNNT based TFTs exhibit higher field-effect mobilities than its originating semiconductor *i.e.* DNNT.

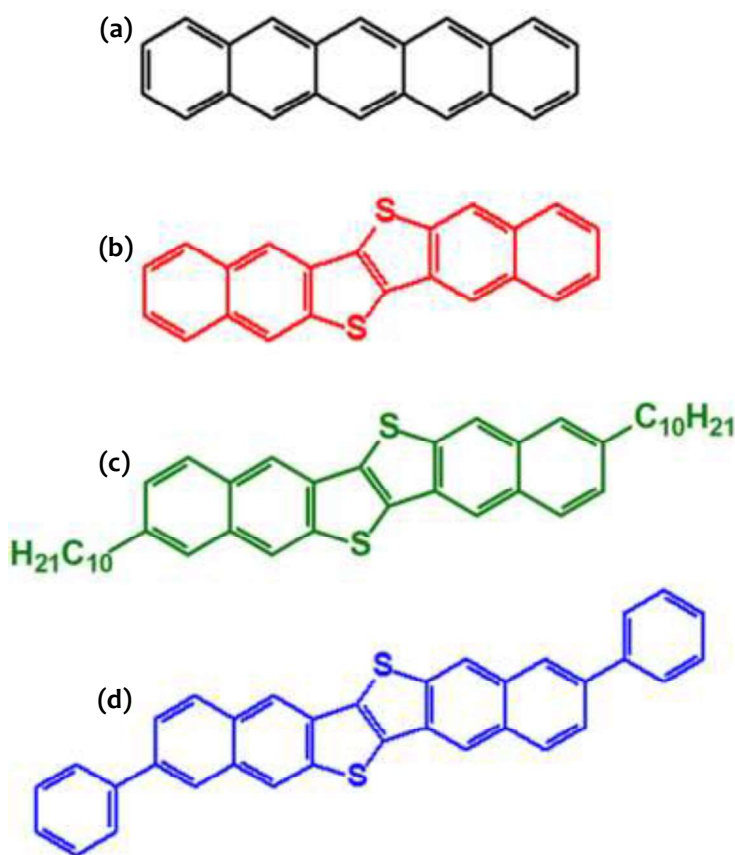


**Figure 3.3** :Chemical structures of Hole-transport Organic Semiconductors Investigated in this Study: (a) Pentacene, (b) DNNT, (c) C<sub>10</sub>-DNNT and (d) DPh-DNNT

The chemical structure of DPh-DNNT is given in Figure 3.3(d). The synthesis of DPh-DNNT and TFTs with this semiconductor are reported in year 2011 for which the field-effect mobility of 3-4 cm<sup>2</sup>/Vs on ODTS treated Si/SiO<sub>2</sub> substrates was extracted [Niimi *et al*, 2011]. This semiconductor has an energy gap of ~3eV and HOMO energy level ~5.3 eV [Kang *et al*, 2013]. The DPh-DNNT based TFTs shows excellent thermal stability as compared to parent semiconductor *i.e.* DNNT and decyl derivatives on both n<sup>+</sup>-Si/SiO<sub>2</sub> and flexible plastic substrates at 250°C [Kang *et al*, 2013; Yokota *et al*, 2013]. On flexible plastic substrates, the TFTs with this semiconductor exhibit a field-effect mobility of 1.9 cm<sup>2</sup>/Vs [Yokota *et al*, 2013]. The DPh- DNNT TFTs exhibits field-effect mobilities higher than the TFTs with originating semiconductor *i.e.* DNNT, but lower than the C<sub>10</sub>-DNNT based TFTs.

Pentacene used for the experiments in this work was purchased from Sigma Aldrich. DNNT and its derivatives C<sub>10</sub>-DNNT and DPh-DNNT were kindly provided for research by the group of Prof. Kazuo Takimiya, who is presently at RIKEN Center for Emergent Matter Science in Japan. The organic semiconductor DNNT is also commercially available now from Sigma Aldrich. However, C<sub>10</sub>-DNNT and DPh-DNNT are not commercially available yet.

### 3.2.2 Electron-transport Semiconductors

The two electron-transport organic semiconductors used are hexadecafluorocopperphthalocyanine abbreviated as  $F_{16}CuPc$  [Bao *et al.*, 1998] and *N,N'*-bis-(heptafluorobutyl)-2,6-dichloro-1,4,5,8-naphthalene tetra-carboxylic diimide [NTCDI or NTCDI- $Cl_2-(CH_2C_3F_7)_2$ ] [Oh *et al.*, 2010] and their chemical structures are given in Figure 3.4.

The barrier for charge injection from source metal to semiconductor is high for electron-transport organic semiconductors due to higher gap between metal Fermi level and LUMO level as compared to the gap between metal Fermi level and HOMO level of hole-transport semiconductors.  $F_{16}CuPc$  for this study was purchased from Sigma Aldrich, whereas NTCDI was provided by BASF SE, Ludwigshafen, Germany.

$F_{16}CuPc$  is one of the first semiconductors developed as electron-transport material in organic devices. This semiconductor shows good air stability owing to its large electron affinity [Ling and Bao, 2006].  $F_{16}CuPc$  has an energy gap of  $\sim 1.7$  eV and LUMO energy level of  $\sim 3.5$  eV. The field-effect mobility of  $0.02$   $cm^2/Vs$  has been achieved for  $F_{16}CuPc$  based organic TFT on Si/SiO<sub>2</sub> substrates as early as 1996 [Bao *et al.*, 1996]. This field-effect mobility has been enhanced to  $0.03$   $cm^2/Vs$  on improving the interface by SAM treatment of SiO<sub>2</sub> dielectric [de Oteyza *et al.*, 2005]. The field-effect mobility of  $F_{16}CuPc$  is highly dependent on the substrate temperature (during deposition of active layer) and thickness of the film [Ye *et al.*, 2009; Oh *et al.*, 2010]. On flexible plastic substrates,  $F_{16}CuPc$  based TFTs have shown field-effect mobility values of  $0.01$   $cm^2/Vs$  with a thin dielectric of AlO<sub>x</sub> treated with a SAM layer [Sekitani *et al.*, 2010].

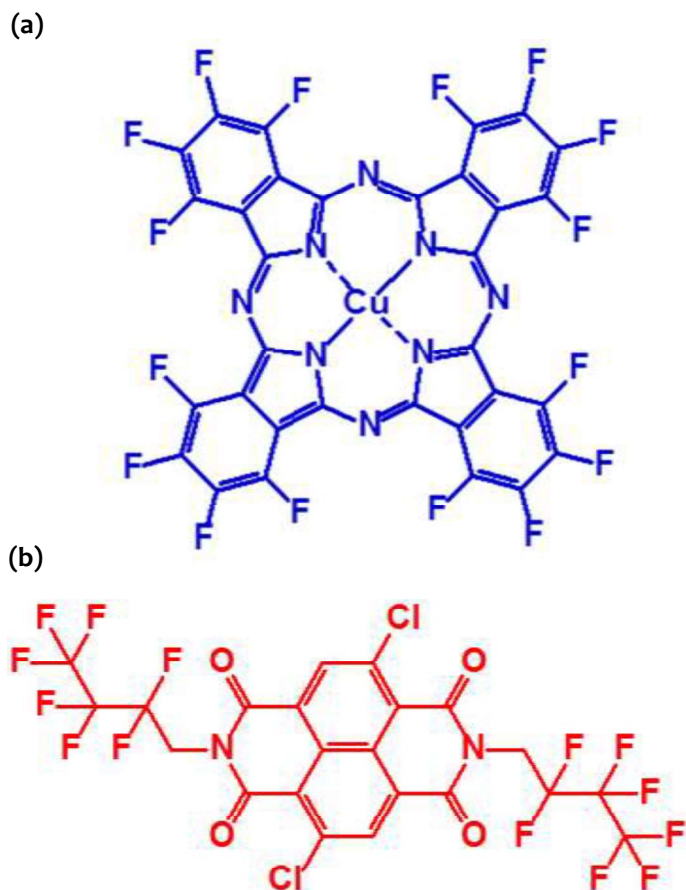


**Figure 3.4** :Chemical structures of Electron-transport Organic Semiconductors: (a)  $F_{16}CuPc$  and (b) NTCDI

NTCDI is one of the recently reported air-stable organic semiconductors [Katz *et al*, 2000; Stolte *et al*, 2010] for electron-transport material in organic devices. This semiconductor has LUMO energy level of  $\sim 4.0$  eV and energy gap of  $\sim 2.0$  eV. The largest field-effect mobility of  $1.3 \text{ cm}^2/\text{Vs}$  is reported for NTCDI based TFTs on Si substrate with a thick gate-dielectric layer consisting of 100 nm-thick  $\text{SiO}_2$ , 8 nm of  $\text{Al}_2\text{O}_3$ , and 1.7 nm-thick SAM [Stolte *et al*, 2010]. The low voltage operation (3.0 V) and a high field effect mobility of  $\sim 0.8 \text{ cm}^2/\text{Vs}$  is achieved for NTCDI TFTs using a thin gate dielectric of  $\text{AlO}_x$  (3.6 nm-thick plasma grown) and SAM (1.7 nm-thick) on heavily doped Si substrate [Rödel *et al*, 2013].

### 3.3 FABRICATION PROCESS

The patterning of different layers of organic TFT was done using four levels of polyimide shadow masks. Shadow masks are made from the thin sheets of metal or polyimide into which openings of structures are made by a high-energy of laser beam. The spot size of the laser limits the resolution of these shadow masks. These masks are usually compatible with various substrates such as glass, plastic, and silicon. The photograph of a polyimide shadow mask used for depositing the source and drain electrode layer is shown in Figure 3.5, and they were purchased from CADiLAC Laser, Hilpoltstein, Germany.



**Figure 3.5** :Photograph of a Polyimide Shadow Mask Used in Deposition Process

For the fabrication, firstly, PEN substrates were pre-heated at  $120^\circ\text{C}$  for one hour to avoid any shrinking/expansion or change in substrate shape and dimensions during deposition process. The substrates were cleaned using acetone, DI water and 2-propanol solutions, and then dried using nitrogen gas before depositing any layer. The step-by-step fabrication process of the organic TFTs is shown schematically in Figure 3.6.

To define the gate electrode, a 30-nm-thick aluminum was deposited at a rate of  $10\text{-}12 \text{ \AA}/\text{sec}$  by thermal vacuum evaporation technique, with a base pressure of  $10^{-6}$  mbar through a polyimide shadow mask. In order to prevent the aluminium gate electrode from being oxidized, connecting pads of aluminium gate electrodes were covered by 20-nm thick gold which was thermally evaporated at a rate of  $0.25\text{-}0.4 \text{ \AA}/\text{sec}$  with a base pressure of  $10^{-7}$  mbar by using the second level of shadow mask. The photograph of the vacuum evaporation system used for depositing the thin films of metal and organic semiconductor is shown in Figure 3.7 (photograph taken in the Organics Electronics Lab, Max Planck Institute for Solid State Research, Germany). The aluminium metal which was not covered with gold was oxidized by briefly exposing the aluminium surface of the substrate to an oxygen plasma for 30 seconds (200 W power and 0.17 mbar base pressure) to form a 3.6-nm thick  $\text{AlO}_x$  layer [Klauck *et al*, 2007;

Sekitani *et al*, 2010]. Oxygen plasma technique increases the native  $\text{AlO}_x$  layer and it also increases the density of hydroxyl (-OH) groups at the surface which helps in condensation of any self-assembled layer over the  $\text{AlO}_x$  surface. This  $\text{AlO}_x$  layer passivated with an ultra-thin (1.7-nm thick) SAM of  $\text{HC}_{14}\text{-PA}$  was used as a gate dielectric.

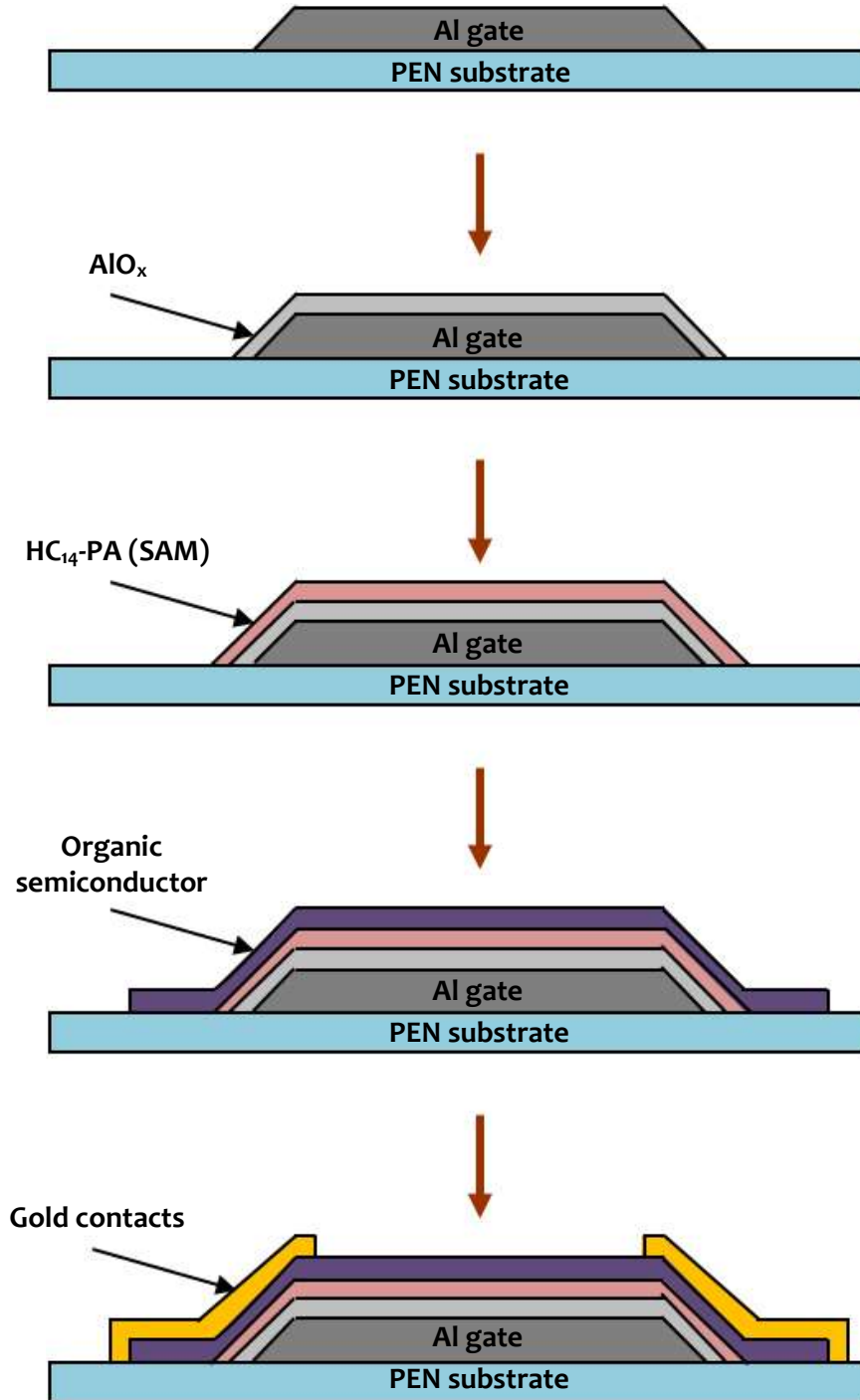


**Figure 3.6 :** Schematic diagram showing the step-by-step Fabrication Process of Organic TFTs on Flexible Plastic Substrates

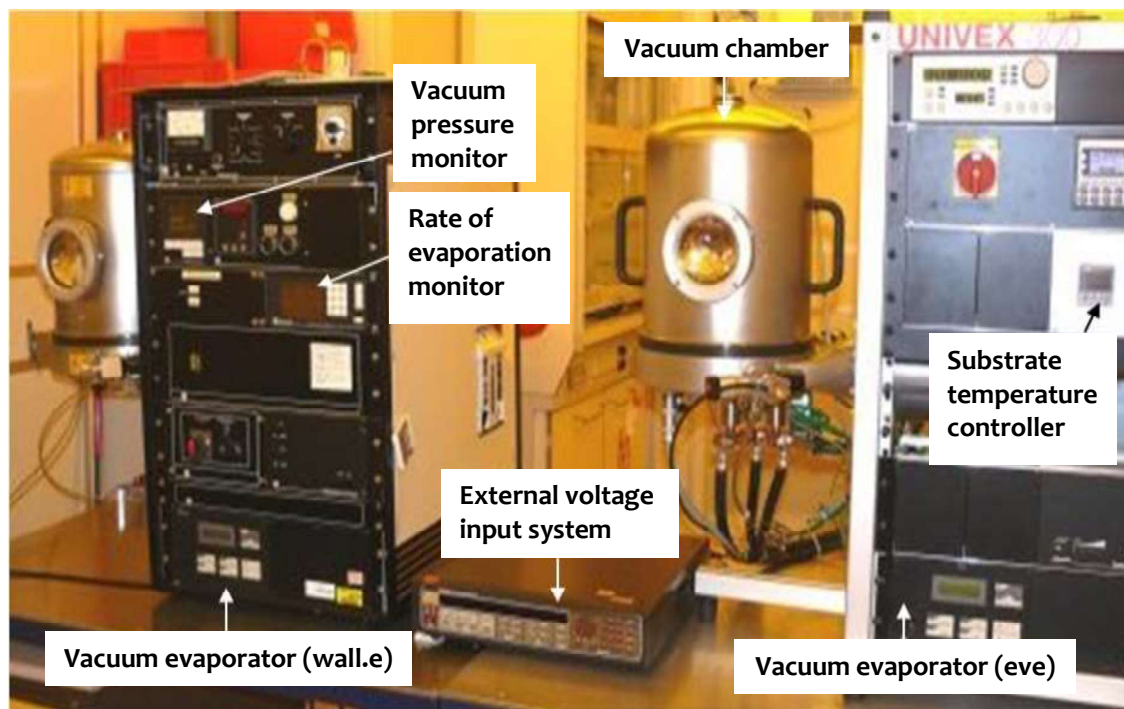


**Figure 3.7 :**Photograph of the Two Vacuum Evaporation System Used for Depositing Metal and Organic Semiconductor Films

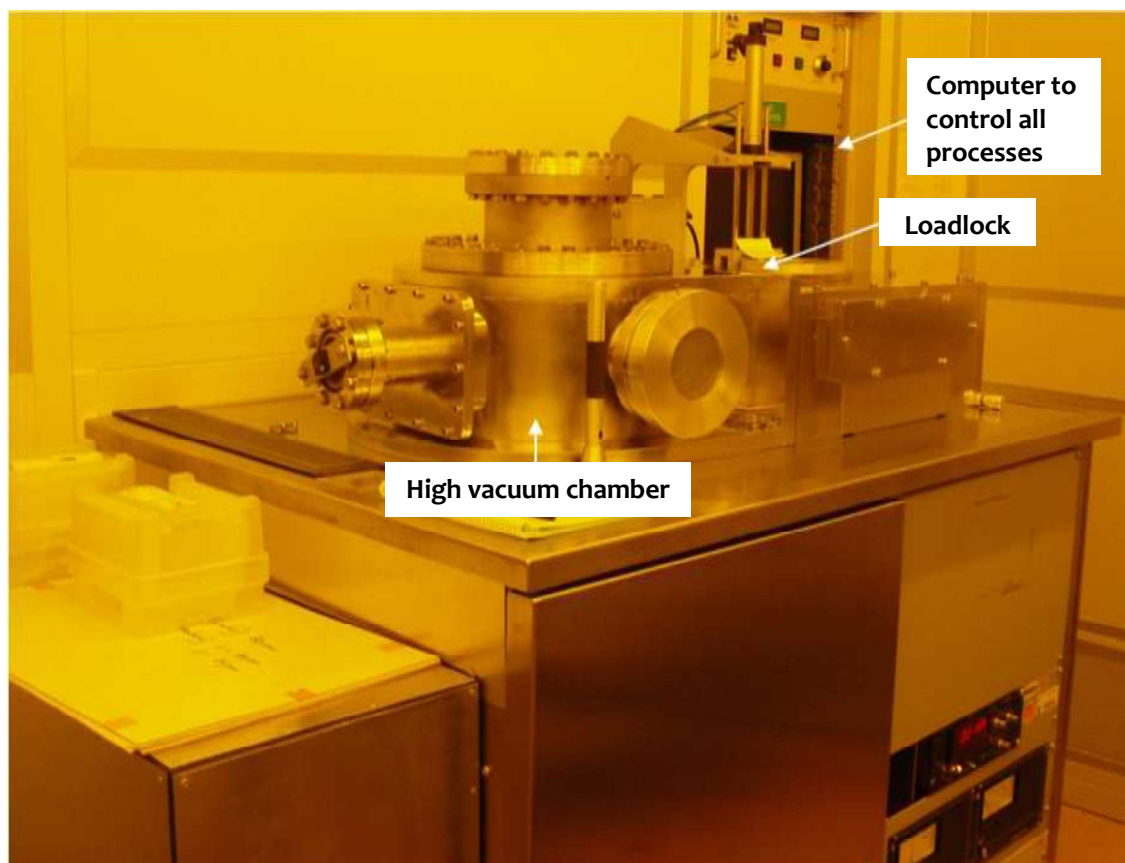


**Figure 3.8 :**Photograph of the Oxygen Plasma System Used for Growing Thin-layer of Dielectric



Tetradecylphosphonic acid used to form SAM as part of the ultrathin gate dielectric was purchased from PCI Synthesis, Newburyport, MA, USA [Ante *et al*, 2011; Zschieschang *et al*, 2012; Fukuda *et al*, 2009; Aghamohammadi *et al*, 2015; Kraft *et al*, 2010; Zschieschang *et al*, 2009; Kraft *et al*, 2014]. The photograph of the oxygen plasma chamber used for growing the thin-film of  $\text{AlO}_x$  is shown in Figure 3.8 (photograph taken in the Organics Electronics Lab, Max Planck Institute for Solid State Research, Germany). The SAM layer was obtained by immersing the substrate into a 2-propanol solution of the phosphonic acid for at least an hour followed by a brief rinsing of the flexible substrate with the 2-propanol solution and then the sample was dried using the nitrogen gas dryer. The chemical structure of  $\text{HC}_{14}\text{-PA}$  is shown in Figure 3.1 and the reason for using the layer of  $\text{HC}_{14}\text{-PA}$  SAM was to reduce the leakage current density through the thin layer of  $\text{AlO}_x$  and to improve the interface between the gate dielectric and the organic semiconductor films which eventually help to achieve a high charge-carrier mobility because this gate dielectric has a low surface energy of  $20 \text{ J/m}^2$  [Klauk, 2010; Zschieschang *et al*, 2010; Ante *et al*, 2011]. The use of  $\text{HC}_{14}\text{-PA}$  SAM also makes the surface of the gate dielectric hydrophobic, which decreases the hysteresis in the electrical characteristics of organic TFTs [Woo Jin *et al*, 2007]. The  $\text{HC}_{14}\text{-PA}$  SAM does not condensate on a gold surface which eventually helps to probe the aluminum gate contacts. The small thickness (5.3 nm) and large capacitance per unit area ( $600 \text{ nF/cm}^2$ ) [Zaki *et al*, 2014], of the  $\text{AlO}_x/\text{SAM}$  gate dielectric allow the transistors and circuits to operate with low voltages of about  $\pm 3.0 \text{ V}$  for both p-channel and n-channel TFTs.

In the next step, the organic semiconductor layer with a thickness of 20 to 30 nm with a rate of  $0.2\text{-}0.3 \text{ \AA/sec}$  and base pressure of  $\sim 10^{-6}$  mbar was deposited onto the  $\text{AlO}_x/\text{SAM}$  gate dielectric by sublimation in vacuum through shadow mask for semiconductor patterning. The vacuum evaporation technique is suitable for the deposition of small molecules to form multicrystalline semiconductor thin-films, thereby improving the charge-transport in the devices. The maximum temperature during the TFT fabrication with various semiconductors was between  $60 \text{ }^\circ\text{C}$  (pentacene) and  $90 \text{ }^\circ\text{C}$  (NTCDI), which was the substrate temperature during semiconductor deposition (see Table 3.1). The substrate temperature enables the organic semiconductor to form a well-ordered film which helps in fabricating organic TFTs with high charge-carrier mobility [Knipp *et al*, 2003]. Finally, a 30-nm thick gold layer was deposited at a rate of  $0.3\text{-}0.4 \text{ \AA/sec}$  and base pressure of  $\sim 10^{-6} - 10^{-7}$  mbar by vacuum evaporation through another shadow mask to define the source and drain contacts of the TFTs. Figure 3.9(a) shows the photograph of the fabricated devices on flexible polyethylene substrate. This photograph shows the fabricated set of devices for their capabilities of flexibility and bendability. Figure 3.9(b) shows the zoomed optical micrograph of a single TFT with L of  $30 \text{ }\mu\text{m}$  and W of  $100 \text{ }\mu\text{m}$ . No encapsulation was done for these devices to protect them from ambient conditions.

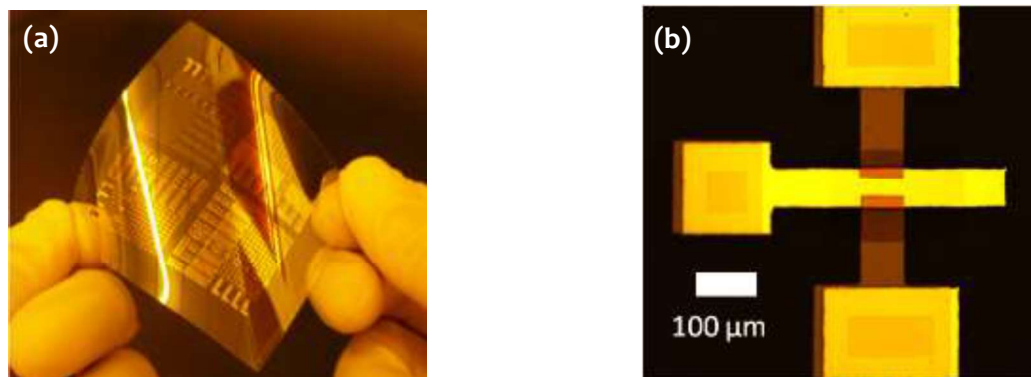


**Figure 3.9** : (a) Photograph of Fabricated Devices on a Flexible Polyethylene Naphthalate Substrates, and (b) Optical Micrograph of an Organic TFT with L of  $30 \text{ }\mu\text{m}$  and W of  $100 \text{ }\mu\text{m}$

### 3.4 ELECTRICAL CHARACTERISTICS

The electrical characterization of the fabricated devices was performed in normal ambient conditions. For all the TFTs, the two important device characteristics *i.e.* output and transfer curves were measured and plotted. To explore the repeatability of characteristics, the effect of multiple cycling of transfer curves was also studied for some of the devices.

#### 3.4.1 Transfer and Output Characteristics

The measured transfer and output characteristics of freshly fabricated flexible p-channel and n-channel TFTs with all six organic semiconductors are discussed in the following Subsections. The important device parameters such as the field-effect mobility, threshold voltage, current on/off ratio, and subthreshold swing are extracted from the transfer plots, as explain in Section 2.4.4.

##### (a) p-channel Organic TFTs

The drain-source current was measured and plotted on y-axis with drain-source or gate-source voltages to obtain the output and transfer characteristics respectively. The output characteristics were plotted for the drain-source voltages continuously varying from 0 V to -3.0 V for a constant gate-source voltage. The gate-source voltage was varied from 0 V to -3.0 V in steps of -0.5 V to find the output curves at different gate voltages. To obtain transfer characteristics, the gate-source voltage was varied continuously from +1.0 V to -3.0 V for a particular drain-source voltage of -3.0 V. The gate current is also included in the transfer plots, to get the estimate of device leakage currents.

The transfer and the output characteristics of pentacene based flexible TFTs are given in Figure 3.10. The output characteristics (right side Figure) show nice linear and saturation regions. The order of the device off-state leakage current *i.e.*  $I_{DS}$  at  $V_{GS} = 0$  V is  $10^{-12}$  A, and the current on/off ratio in range of  $10^7$ . These devices show very low gate leakage current of less than 0.1 pA. The extracted field-effect mobility and the threshold voltage for this pentacene device are  $0.54 \text{ cm}^2/\text{Vs}$  and -1.0 V, respectively. These devices show a low subthreshold swing of 0.1 V/decade. The performance of this device is comparable to the highest values reported in the literature for pentacene-based TFTs fabricated on plastic substrates with same configuration [Ishida *et al*, 2011].

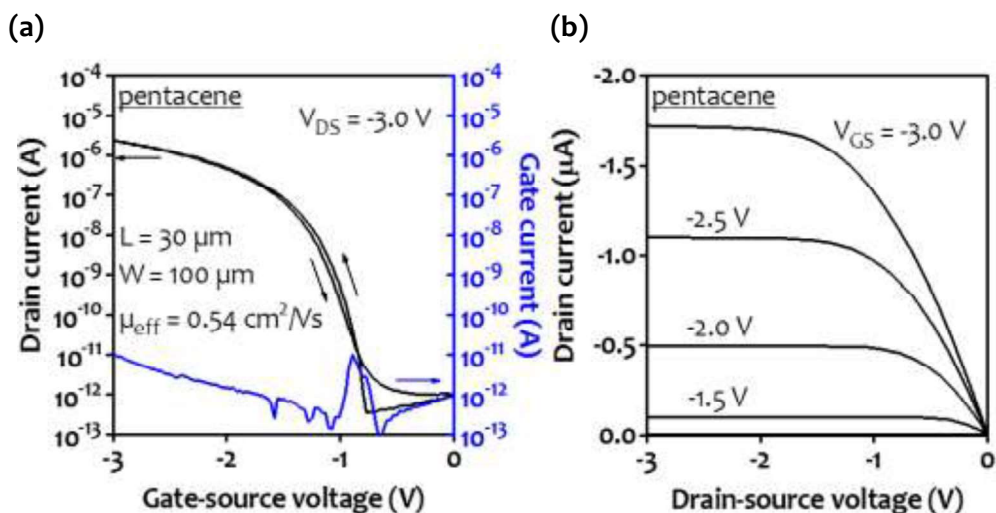


Figure 3.10 : (a) Transfer and (b) Output; Characteristics of a Fresh Pentacene Flexible TFT Measured shortly after the Fabrication

The transfer and output characteristics of DNTT and its derivatives *i.e.* C<sub>10</sub>-DNTT and DPh-DNTT based flexible TFTs are given in Figure 3.11-3.13. These devices show nice linear and saturation behavior in the output characteristics. The DNTT, C<sub>10</sub>-DNTT and DPh-DNTT based TFT devices show the field-effect mobility and threshold voltage values of 1.8 cm<sup>2</sup>/Vs and -1.2 V, 4.1 cm<sup>2</sup>/Vs and 0.4 V, and 1.8 cm<sup>2</sup>/Vs and -0.8 V, respectively. All these devices show very low gate leakage currents (below 10 pA), and device off-state leakage current of order 10<sup>-11</sup>-10<sup>-12</sup> A. For the devices which are not completely switched off at zero gate-source voltage (p-channel devices with positive threshold voltage), the lowest current in the completely off condition is taken as off state current. This happens for C<sub>10</sub>-DNTT devices. These devices show high current on/off ratios of ~10<sup>7</sup>, ~10<sup>8</sup>, and ~10<sup>7</sup> respectively for DNTT, C<sub>10</sub>-DNTT and DPh-DNTT based TFTs.

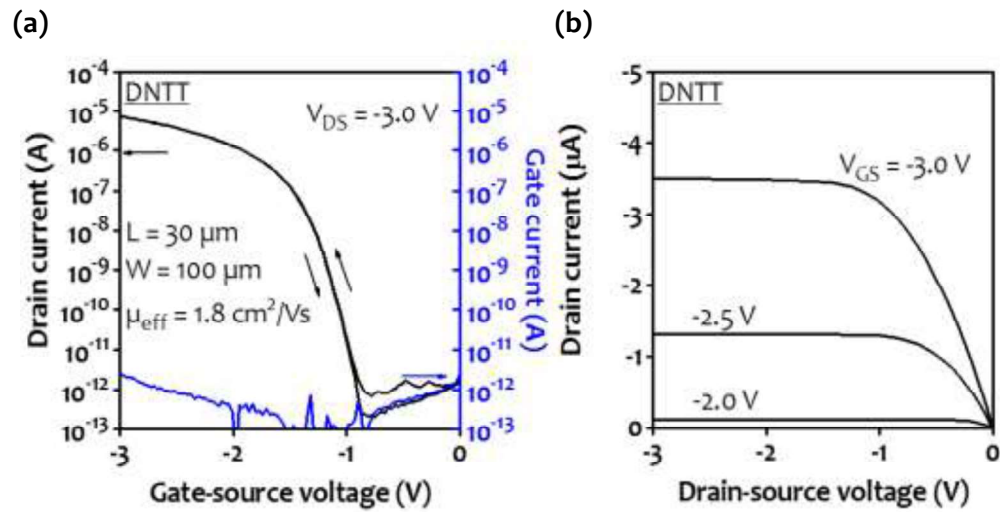


Figure 3.11 : (a) Transfer and (b) Output; Characteristics of a Fresh DNTT Flexible TFT Measured shortly after the Fabrication

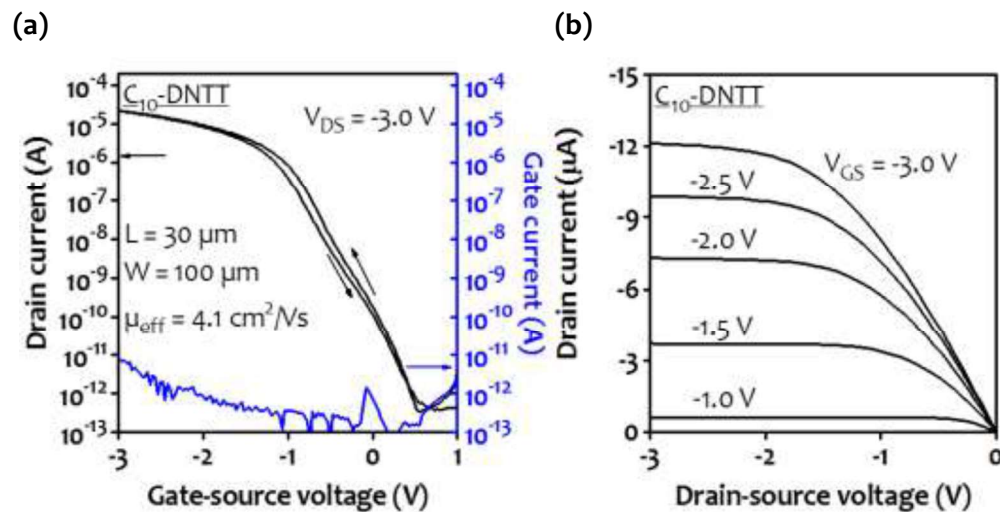
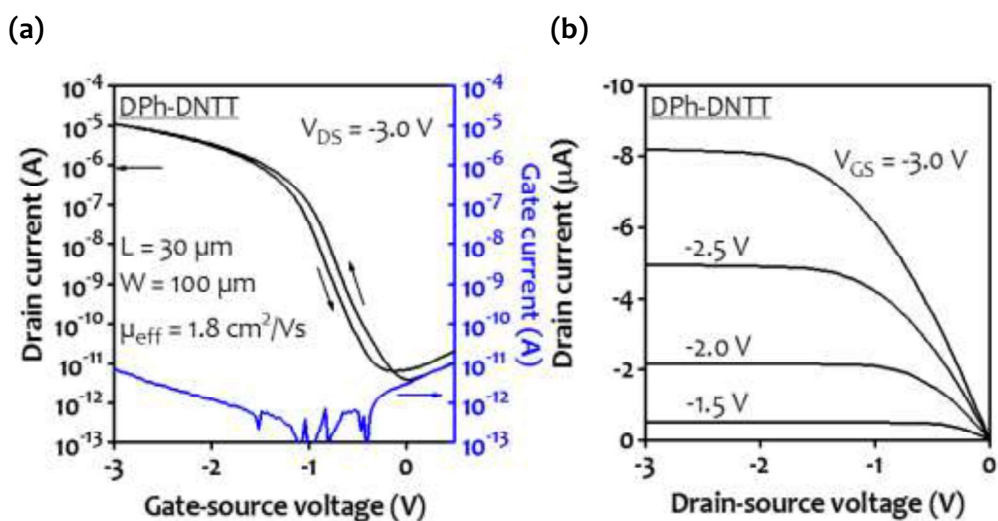


Figure 3.12 : (a) Transfer and (b) Output; Characteristics of a Fresh C<sub>10</sub>-DNTT Flexible TFT Measured shortly after the Fabrication



**Figure 3.13 :**(a) Transfer and (b) Output; Characteristics of a Fresh DPh-DNTT Flexible TFT Measured shortly after the Fabrication

The DNTT based TFTs show the subthreshold swing of 0.1 V/decade, which is the lowest among all the fabricated TFTs. The field effect mobility achieved by DPh-DNTT based TFTs are higher than the originating semiconductor *i.e.* DNTT, but less as compared to C<sub>10</sub>-DNTT based TFTs. The C<sub>10</sub>-DNTT devices show very high current on/off ratio, which is highest among all the p-channel and n-channel TFTs fabricated for this work. The performance of the fabricated devices are similar to the highest reported values of DNTT, C<sub>10</sub>-DNTT, and DPh-DNTT which are available in literature using the same structure of TFT [Zschieschang *et al*, 2011; Zschieschang *et al*, 2012; Yokota *et al*, 2013]. However, DPh-DNTT being a relatively new semiconductor, further exploration of its properties in TFT devices is essential.

### (b) n-channel Organic TFTs

Figure 3.14 and 3.15 show the measured transfer and output characteristics of F<sub>16</sub>CuPc and NTCDI flexible TFTs, respectively. The output characteristics were plotted for the drain-source voltages continuously varying from 0 V to +3.0 V for a particular gate-source voltage. The gate-source voltage was varied from 0 V to +3.0 V in steps of +0.5 V to find the output curves at different gate voltages. To obtain transfer characteristics, the gate-source voltage was varied continuously from -1.0 V to +3.0 V for a particular drain-source voltage of +3.0 V.

The field-effect mobilities and threshold voltage extracted from the transfer characteristics are 0.03 cm<sup>2</sup>/Vs and +0.1 V for the F<sub>16</sub>CuPc based TFTs; and 0.16 cm<sup>2</sup>/Vs and +0.2 V for the NTCDI based TFTs, respectively. The NTCDI based TFTs show the device off-state leakage current of 10<sup>-13</sup> A, which is lowest among all reported devices in this work; and current on/off ratio of the order 10<sup>7</sup>. Both F<sub>16</sub>CuPc and NTCDI TFTs show low gate leakage currents (below 10 pA) and subthreshold swing of 0.2 V/decade and 0.1 V/decade, respectively. The performance parameters of these devices are comparable to the highest values reported in the literature for F<sub>16</sub>CuPc and NTCDI based TFTs with same configuration [Ishida *et al*, 2011; Yang *et al*, 2015; Rödel *et al*, 2013]. However, NTCDI being a relatively new semiconductor, further exploration of its properties in TFT devices is very essential.

Table 3.1 summarizes the electronic properties (HOMO level, LUMO level, and energy gap) of all the investigated organic semiconductors, process temperature, and the extracted device parameters from fabricated TFTs, such as field-effect mobility, current on/off ratio, subthreshold swing, transconductance, and threshold voltage.

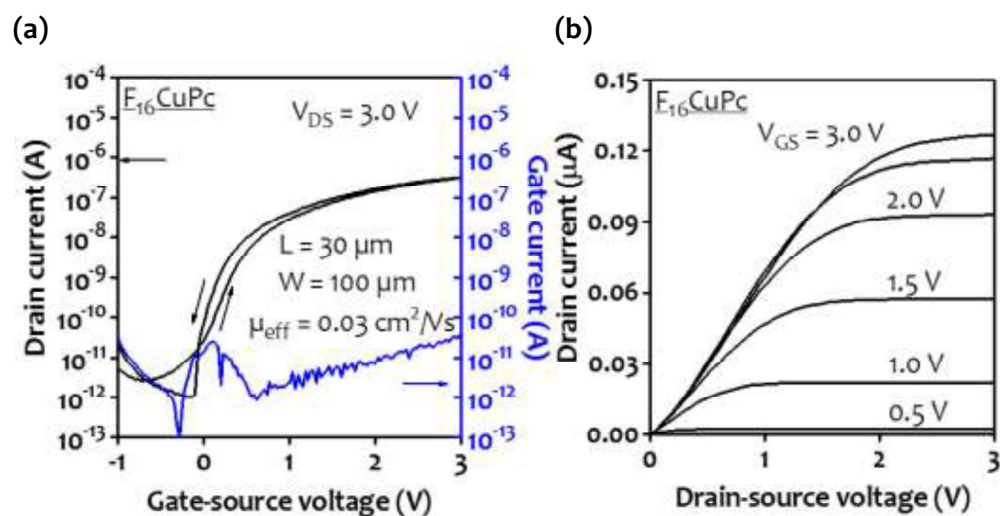


**Figure 3.14** : (a) Transfer and (b) Output; Characteristics of a Fresh  $F_{16}CuPc$  Flexible TFT Measured shortly after the Fabrication

**Table 3.1** : Extracted Values of Field-effect Mobility, Threshold Voltage, Current on/off Ratio, and Subthreshold Swing of Flexible p-channel and n-channel TFTs using Six Different Organic Semiconductors Investigated in this Study

Semiconductor	pentacene	DNTT	$C_{10}$ -DNTT	DPh-DNTT	$F_{16}CuPc$	NTCDI
Carrier type	p-channel TFT	p-channel TFT	p-channel TFT	p-channel TFT	n-channel TFT	n-channel TFT
HOMO level (eV)	~5	~5.44	~5.38	~5.4	~5.2	~6
LUMO level (eV)	~3	~2.44	~2.38	~2.4	~3.5	~4
Energy gap (eV)	~2	~3	~3	~3	~1.7	~2
Process temperature	60 °C	60 °C	80 °C	80 °C	90 °C	65 °C
Field-effect mobility	0.5	1.8	4.1	1.8	0.03	0.16
Threshold voltage	-1.0	-1.2	0.4	-0.8	0.1	0.2
Current on/off ratio	$10^7$	$10^7$	$10^8$	$10^7$	$10^6$	$10^7$
Subthreshold swing	0.1	0.1	0.2	0.2	0.2	0.1

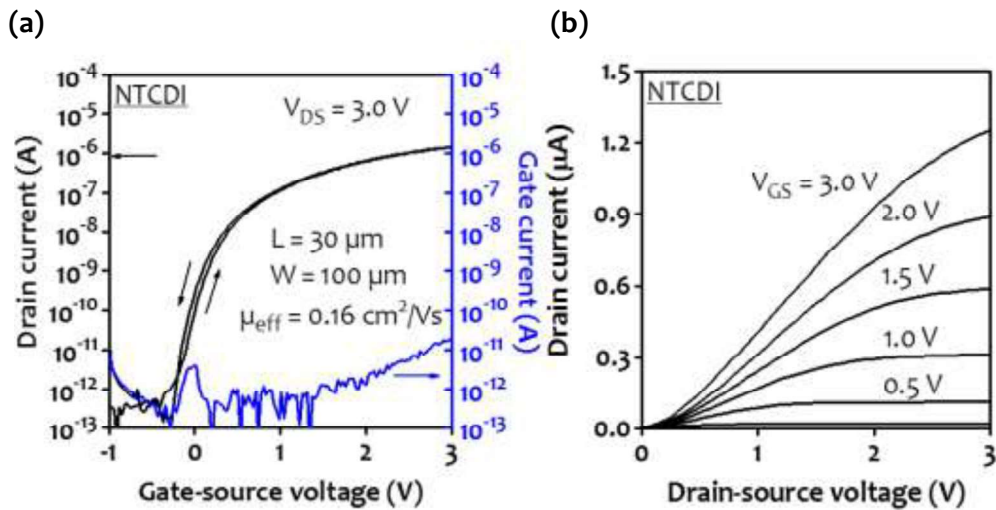


**Figure 3.15 :**(a) Transfer and (b) Output; Characteristics of a Fresh NTCDI Flexible TFT Measured shortly after the Fabrication

### 3.4.2 Multiple Scans

Repeatability of electrical characteristics upon multiple operations is very important for the deployment of the organic TFTs in flexible electronic circuitry, which is comprehensively studied for the fabricated flexible TFTs. The operational stability upon repeated scans is essential to evaluate the stability and reliability of the devices. Measuring the multiple scans of transfer characteristics is one of the expected methods to explore the repeatability of characteristics of TFT devices [Kagan *et al*, 2005; Mathijssen *et al*, 2007; Sirringhaus, 2009; Zhang *et al*, 2009].

There are various reports available in literature on operational stability of organic TFTs on multiple repeated scans of the transfer characteristics [Kagan *et al*, 2005; Tiwari *et al*, 2009; Zhang *et al*, 2009; Ahmed *et al*, 2012; Zhou *et al*, 2013]. However, most of these reports, demonstrate the results for less number of scans and/or for TFTs fabricated on rigid Si substrates. Such studies on flexible low-voltage devices are scarce, especially with acute conditions of repeatability, which is crucial for real-life conditions. Hence, for any high performance flexible TFT device, studying the repeatability for large number of scans is essential.

To study for a real scenario, where high-performance flexible TFTs have to operate for many hours and also switched on/off for hundreds of times, TFTs with DPh-DNTT were continuously scanned for multiple transfer characteristics for a long duration. In this measurement, transfer characteristics were measured repeatedly for multiple times (up to 1985 scans) for duration of 10 hours to provide an acute condition for evaluating the operational stability of the devices. This time includes both the times taken for the forward and the reverse sweep, however, the forward transfer characteristics are used for extracting the device parameters. The effect of the multiple scans of transfer characteristics on the performance of the TFT devices, specifically the changes in the important performance parameters such as field-effect mobility, threshold voltage, current on/off ratio, subthreshold swing, and the off state leakage current are studied here.

The plot of multiple transfer characteristics of flexible DPh-DNTT TFTs is given in Figure 3.16. It can be clearly seen from the transfer plots that the threshold voltage shifts in negative

direction, off current increases, and current on/off ratio decreases upon continuously scanning the transfer characteristics.

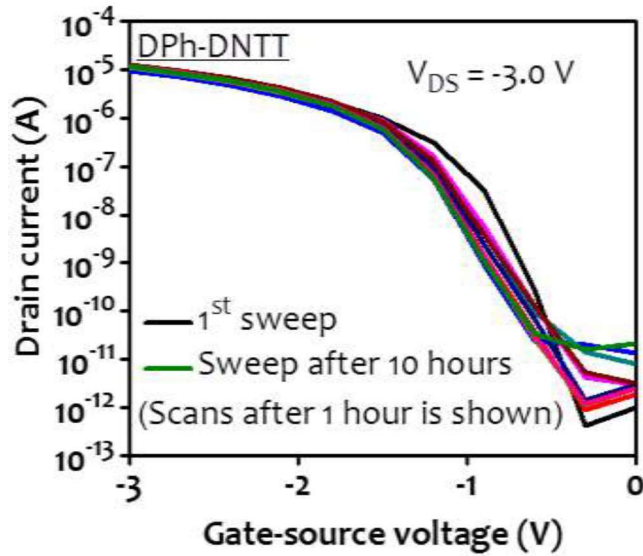


**Figure 3.16** : Effect of Multiple Scans on the Transfer Characteristics of TFTs based on DPh-DNTT Semiconductor; Black and Green Curves Indicate the plots of 1<sup>st</sup> and 1985<sup>th</sup> Scan (Last Scan after 10 Hours), respectively

Figure 3.17(a) shows the variation of the threshold voltage with time. The shift in threshold voltage is maximum in initial scans (from -0.8 V to -1.1 V), however threshold voltage value saturates after initial few hours of continuous multiple scans. The field-effect mobility is extracted from the multiple scan transfer characteristic curves and is plotted in Figure 3.17(b). The field-effect mobility increases from 1.7 cm<sup>2</sup>/Vs during initial sweeps, and saturates later at 2.1 cm<sup>2</sup>/Vs. Hence, an increase in mobility is seen which is suspected to be due to the molecular rearrangements in the semiconductor film, or due to the reduction in contact resistance reduction which eventually improves the performance of devices [Kalb *et al*, 2007; Lu *et al*, 2011].

Apart from the total duration of continuous scans of transfer characteristics, it is also important to analyze how many times each device was switched on or off to know the life time of the device for number of operations continuously. Hence, the parameters with respect to the number of scans are summarized in Table 3.2.

**Table 3.2** :Extracted Field-effect Mobility Values, Threshold Voltage, Off current, Current on/off Ratios with Number of Scans for Flexible DPh-DNTT TFTs

Time (#Scan)	Field-effect mobility (cm <sup>2</sup> /Vs)	Threshold voltage (V)	I <sub>OFF</sub> (A)	I <sub>ON</sub> /I <sub>OFF</sub>
1 min (#1)	1.7	-0.8	~10 <sup>-12</sup>	10 <sup>7</sup>
120 min (#500)	1.9	-1.0	~10 <sup>-12</sup>	10 <sup>7</sup>
600 min (#1985)	2.1	-1.0	~10 <sup>-11</sup>	10 <sup>6</sup>

As it can be seen from this table, up to about 500 scans, the off current ( $I_{OFF}$ ) and current on/off ratio ( $I_{ON}/I_{OFF}$ ) are almost constant, and as high as  $10^7$ . However, the  $I_{OFF}$  increases from the order of  $10^{-13}$  to  $10^{-12}$  A, when number of scans reach to 1985. The same can be observed in Figure 3.16 also. This increase in the off current results in the reduction of current on/off ratio from  $10^8$  to  $10^7$ , which is undesirable.

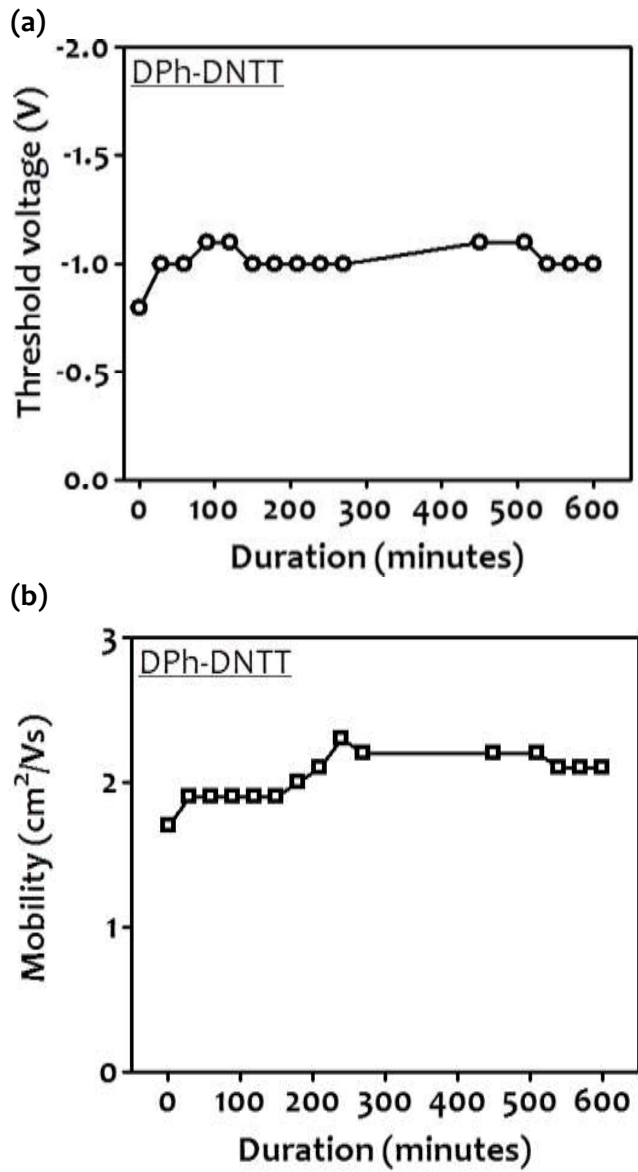


**Figure 3.17** :Changes in (a) Threshold Voltage, and (b) Field-effect Mobility Extracted from the Transfer Characteristic of DPh-DNTT TFT due to Multiple Continuous Scans for 10 Hours on the Same Device

This study shows that DPh-DNTT TFTs show high operational stability for continuous scans for more than thousand scans. Even after the acute conditions for continuous operation for 600 minutes, these TFTs have shown high stability in device performance, where the threshold voltage and field-effect mobility value change by 20% and 30% respectively. The current on/off ratio do not degrade by more than one order of magnitude, which changes from  $10^7$  to  $10^6$ , which is still very high for switching and low power applications.



### 3.5 SHELF-LIFE STABILITY STUDY

Study of shelf-life stability in organic TFTs is very important for quantifying the degradation of electrical properties of device with time, especially the degradation of electronic properties of organic semiconductors upon exposure to environmental conditions. It has been observed that the performance of organic TFTs degrade on exposure to air, due to the oxidation of the organic material [Zschieschang *et al*, 2011]. The presence of the oxygen, water vapor, ozone, light, and moisture in the environment results in loss of conjugation of organic material which are often the main reason for the degradation of the electronic properties on exposure to air [Ling *et al*, 2007; Zschieschang *et al*, 2012]. Due to different chemical structures, each organic semiconductor will show different amount of degradation on exposure to air. The shelf-life stability is generally studied by measuring the output and transfer curves of devices with time when they are left in normal ambient air with oxygen, moisture, and any other molecule/gas present in the environment where fabricated devices are stored or deployed. The changes in electrical characteristics are observed with time, especially the shift in threshold voltage, change in field-effect mobility, and increase/decrease in on and off currents, all of which are extracted from transfer curves.

It is essential to have an organic semiconductor which is stable in TFTs and leads to reliable operation over time. Hence, it is extremely important to examine the shelf-life stability of high performing TFT devices, to know their applicability for longer durations in real life conditions. In this work, the shelf life study for the relatively new organic semiconductors *i.e.* DPh-DNTT for p-channel, and NTCDI for n-channel; based TFTs is presented. Both of these semiconductors exhibit decent field effect mobility values of  $1.8 \text{ cm}^2/\text{Vs}$  and  $0.16 \text{ cm}^2/\text{Vs}$  for a p-channel and n-channel organic TFT; and it is interesting to see the stability of these TFTs on exposure to ambient conditions. As, there are no studies in literature regarding the stability of these TFTs on exposure to air, these TFTs were exposed to ambient conditions with yellow light (laboratory conditions) and humidity of about 40-50%. The transfer and output characteristics of these TFTs were measured occasionally with an interval of one to few days in between, during the exposure to ambient conditions.

#### 3.5.1 DPh-DNTT based Organic TFTs

The transfer and output characteristics of DPh-DNTT based flexible TFT device, upon exposure to air for 40 days is given in Figure 3.18.

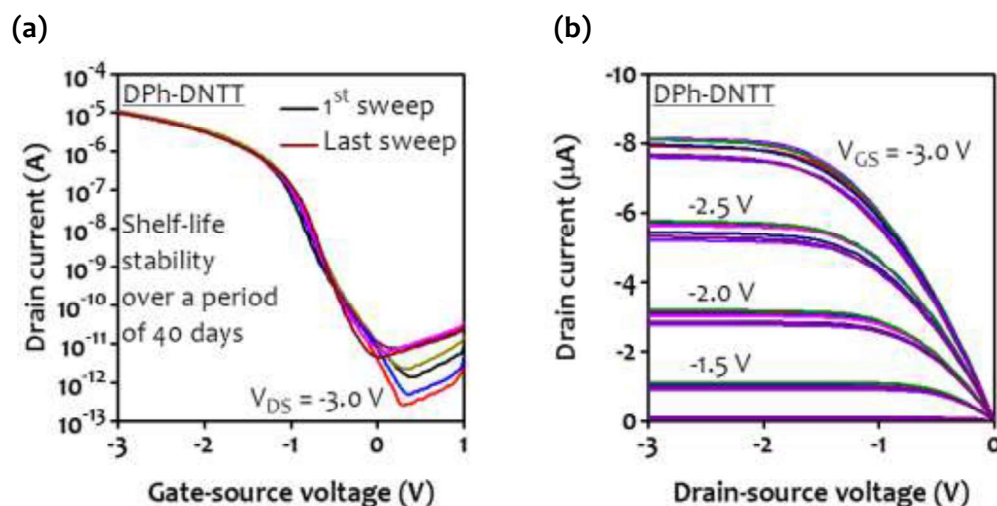


**Figure 3.18 :** (a) Transfer, and (b) Output; Curves of DPh-DNTT TFTs, Measured occasionally with a Period of a Day or Few Days for 40 Days, showing the Changes in Electrical Characteristics, upon Exposure to Ambient Conditions

It has been observed that extracted field-effect mobility changes less than 15% for these devices *i.e.* from 1.8 cm<sup>2</sup>/Vs to 1.6 cm<sup>2</sup>/Vs. The change in the threshold voltage *i.e.* from -0.8 V and change in subthreshold swing *i.e.* from 180 mV/decade remain insignificant in these devices after exposure to air for 40 days. The device off state leakage current increases slightly; thereby reducing the current on/off ratio from 10<sup>8</sup> to 10<sup>7</sup>, during exposure of these TFTs in ambient conditions. The device characteristics of DPh-DNTT based TFTs are very similar even after, exposure of these TFTs to ambient conditions for 40 days, showing very good shelf-life stability.

### 3.5.2 NTCDI based Organic TFTs

The transfer and output characteristics of the NTCDI flexible TFT device upon exposure to air for 10 days, is given in Figure 3.19. The device characteristics show slight variation in the performance of devices on exposure to ambient conditions. The extracted field-effect mobility reduces to less than 20% *i.e.* from 0.16 cm<sup>2</sup>/Vs to 0.13 cm<sup>2</sup>/Vs and threshold voltage changes slightly for NTCDI TFTs on exposure to ambient conditions. The device off state leakage current slightly decreases; however, the current on/off ratio remains in the same order *i.e.* 10<sup>7</sup> during the exposure conditions. The subthreshold swing remains unchanged *i.e.* 110 mV/decade on exposure of these TFTs to ambient conditions. The NTCDI based organic TFTs show good stability on exposure to air for a period of 10 days.

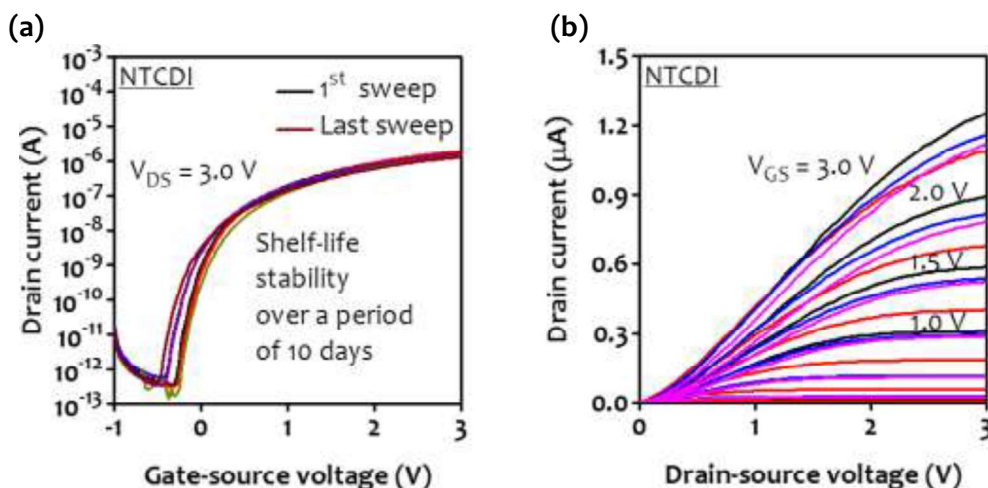


**Figure 3.19** :Plots of (a) Transfer and (b) Output; Curves of the same Flexible NTCDI TFTs, after Exposure to Ambient Conditions for a Period of 10 Days

Similar measurements of stability on exposure to ambient conditions were also performed for other p-channel (pentacene, DNTT, and C<sub>10</sub>-DNTT) and n-channel (F<sub>16</sub>CuPc) organic TFTs demonstrated in this study. The transfer and output characteristics for the mentioned semiconductors were measured occasionally with an interval of a day or few days in between, during exposure of these TFTs to air. Each measurement was performed on different device; however fabricated on the same substrate. The transfer and output characteristics of these devices showing the stability of these TFTs on exposure to ambient conditions is summarized in Appendix A. The shelf-life stability of these TFTs for longer duration is also available in literature. For example, (i) for a pentacene TFT device fabricated using the same architecture for a long duration of 120 days; significant field-effect mobility drop is reported from ~0.7 cm<sup>2</sup>/Vs to less than 0.1 cm<sup>2</sup>/Vs, due to the oxidation of the pentacene films [Zschieschang *et al.*, 2011]; (ii) for longer duration of 240 days of exposure to ambient conditions, field-effect mobility of

DNTT TFTs is reported to decrease from 2.1 cm<sup>2</sup>/Vs to 2.0 cm<sup>2</sup>/Vs in 90 days, and to 1.5 cm<sup>2</sup>/Vs in 240 days, showing good shelf-life stability as compared to pentacene TFTs [Zschieschang *et al*, 2011]; (iii) for C<sub>10</sub>-DNTT based TFTs, field-effect mobility remains well above 2 cm<sup>2</sup>/Vs on exposure to air for a period of 60 days [Zschieschang *et al*, 2012]; and (iv) F<sub>16</sub>CuPc based TFTs show good stability on exposure to air for a period of 10 days, reporting that the degradation of field-effect mobility in F<sub>16</sub>CuPc TFTs is independent of the technique (soft contact lamination or vacuum evaporation) used for deposition [Ling and Bao, 2006].

### 3.6 CONCLUSIONS

The fabrication of high-performing low-voltage p-channel and n-channel organic TFTs on flexible plastic substrates using six different hole-transport and electron-transport organic semiconductors is explained in detail in this Chapter. The output characteristics of all organic TFTs show nice linear and saturation regions. The extracted field-effect mobility from transfer characteristics is in the range of 0.5 cm<sup>2</sup>/Vs to 4.1 cm<sup>2</sup>/Vs for p-channel organic TFTs. The n-channel TFTs based on F<sub>16</sub>CuPc and NTCDI exhibit field-effect mobility values of 0.03 cm<sup>2</sup>/Vs and 0.16 cm<sup>2</sup>/Vs, respectively. The current on/off ratios of p-channel and n-channel organic TFTs are in the range of 10<sup>6</sup> to 10<sup>8</sup>. The performance parameters of all the fabricated organic TFTs are similar to the highest reported values for these semiconductors.

The repeatability study for DPh-DNTT based flexible TFTs upon multiple scans of transfer curves have shown that even after the acute conditions for continuous operation for 10 hours; there is no significant change in the device performance. The threshold voltage and field-effect mobility values change only by 20% and 30% respectively after this 10 hours of scan, whereas the current on/off ratio does not degrade by more than one order of magnitude, changes from 10<sup>7</sup> to 10<sup>6</sup>, still very high for switching and low power applications.

The shelf-life stability studies show that for flexible TFTs with DPh-DNTT, there is a minimal change in the field-effect mobility from 1.8 cm<sup>2</sup>/Vs to 1.6 cm<sup>2</sup>/Vs and threshold voltage remains unchanged throughout the exposure to ambient conditions with humidity of about 40-50%. Overall, these TFTs show very high shelf-life stability. NTCDI based flexible organic TFTs have shown decent shelf-life stability on exposure to air for 10 days, showing a reduction of less than 20% *i.e.* from 0.16 cm<sup>2</sup>/Vs to 0.13 cm<sup>2</sup>/Vs and slight change in threshold voltage on exposure to ambient conditions. These TFTs show good stability on exposure to air for a period of 10 days.

